Experimental Study on Continuous and Oscillatory Rotational Penetration

Yong Tang, S.M.ASCE¹; and Junliang (Julian) Tao, Ph.D., A.M.ASCE²

¹School of Sustainable Engineering and the Built Environment, Arizona State Univ., Tempe.

Email: ytang116@asu.edu

²School of Sustainable Engineering and the Built Environment, Arizona State Univ., Tempe.

Email: julian.tao@asu.edu

ABSTRACT

"Wiggling," rotational and oscillatory motions are often adopted by many living organisms to penetrate into or burrow in the soil. For example, seeds of the Erodium cicutarium and Pelargonium can bury themselves into the ground for future germination with a continuous rotational motion. The angled worm lizards (Agamodon anguliceps) make tunnels by oscillating their head along the long axis of the trunk. Our previous numerical simulations indicate that both rotational modes lead to comparable reductions of penetration resistance of a rod with a conical tip. In this study, both modes of rotational penetration were further investigated through laboratory experiments. The penetrator consists of a cylindrical shaft and a conical tip with an apex angle of 60°. A gear motor is integrated into the penetrator for rotational motion control: both continuous rotation and oscillatory rotation can be achieved. The penetrator assembly is connected to a six-axis robotic arm, which controls the vertical penetration and collects the force/displacement data. A series of rotational penetration tests were conducted in Ottawa sand F65 with different combinations of vertical and rotational velocities while the resultant velocity was kept as a constant. Different oscillation amplitudes were used under the same rotational velocity for the oscillatory rotational penetration cases. The results confirmed the conclusions drawn from the numerical simulations: for both rotational penetration modes, the rotational penetration forces decrease with the relative slip velocity (ratio between the rotational and vertical velocity); comparing with the non-rotational case, the reduction of penetration force is about 80% for the whole-body-continuous-rotation (WCR) case and 60% for the conecontinuous-rotation (CCR) and cone-oscillatory-rotation (COR) when the relative slip velocity reaches 20. Under the tested conditions, the penetration forces were not affected by the oscillation amplitudes. Comparing with continuous rotational penetration, oscillatory penetration achieved less reduction of penetration force, but it is easier to be implemented in cone penetration tests or self-burrowing robots.

INTRODUCTION

In nature, numerous organisms live underground or grow within the soil. The burrowing organisms move in the soil effectively and efficiently by using a wide spectrum of traits. But most burrowing organisms do not penetrate directly using a blunt force. They dynamically change their body shapes so as to wiggle, rotate, undulate, oscillate or expand/contract. These motions lead to a reduction of the penetration resistance, an increase of the thrust and anchorage, or both. For instance, the razor clams (*Ensis directus*) penetrate the wet sand by periodically expanding and contracting its shell and muscular foot (Dorgan 2015; Huang and Tao 2020; Trueman and Yonge 1967; Winter et al. 2014); the sandfish lizards (*Scincus scincus*) undulate its

body to swim through the sandy substrate (Maladen et al. 2009, 2011b; Maladen et al. 2011a); plant roots grow with a circumnutation movement (Migliaccio et al. 2013). It has been found that the seeds of *Erodium cicutarium* and *Pelargonium*, as shown in Fig. 1 (a), can bury themselves into the ground for future germination by cyclically alternating the coiling and uncoiling motion of the bi-layered awn structure (Evangelista et al. 2011; Stamp 1984). The bi-layered structure of the awn, as shown in Fig. 1 (b), can generate the differential deformation when the humidity changes, which will result in the coiling and uncoiling motion. This periodical process leads to a continuous rotational penetration movement of the seed (Abraham and Elbaum 2013a). There are several burrowing mechanisms adopted by the worm lizards (amphisbaenians), as summarized in (Gans 1968). The angled worm lizards (*Agamodon anguliceps*, Fig. 1 (d)) burrow in sandy environment by oscillating their head along the long axis of the trunk (Cogger et al. 1998; Gans 1968), as shown in Fig. 1 (c).

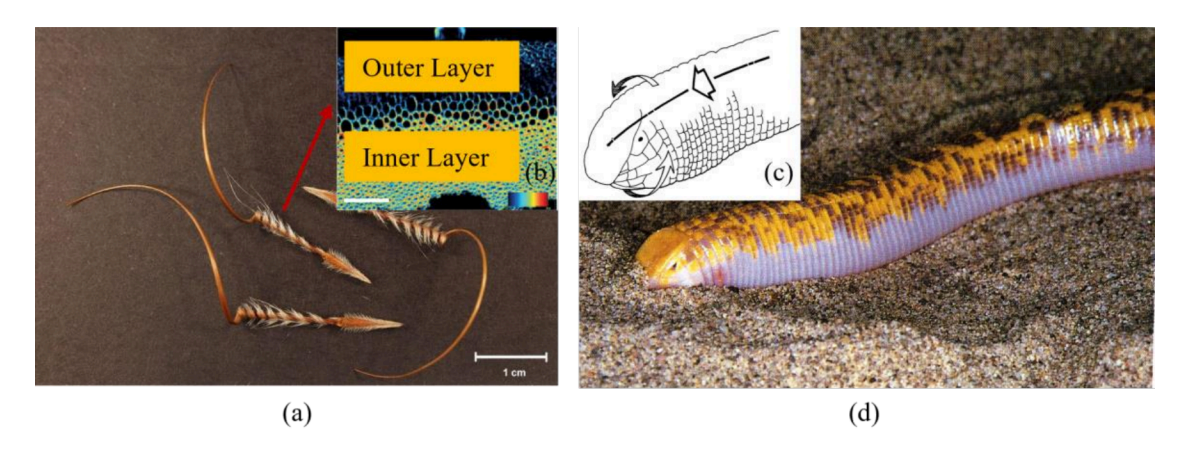


Fig. 1. Bio-inspired models: (a) Seed awn (Image courtesy of the SA Seed Conservation Centre); (b) Bi-layered structure of the awn (modified from (Abraham and Elbaum 2013b)); (c) Oscillatory motion of the head of the worm lizard (adopted from (Cogger et al. 1998)); (d) Trogonophidae (worm lizard, adopted from (Gans 1968))

Both the coiling and uncoiling process by seeds as well as the oscillation motion by worm lizards generate rotational movements. A previous numerical study from the authors (Tang and Tao 2022a; Tang and Tao 2022b) showed that the cone-continuous-rotation (CCR) and the whole-body-continuous-rotation (WCR) could reduce the tip resistance of penetration to a comparable level under the same conditions, while the shaft resistance of the WCR case is lower than that of the WCR case. In this study, the force involved in penetration with no rotation (control), continuous rotation (WCR, CCR) ,and oscillatory rotations (COR) are further investigated through laboratory experiments with a robotic arm and motorized penetrators.

METHODOLOGY

The experimental setup of the rotational penetration test is illustrated in Fig. 2. The penetrator consists of a 20 cm long and 2.5 cm thick cylindrical shaft and a conical tip with an apex angle of 60°. A gear motor is integrated into the penetrator for rotational motion control. WCR testing is conducted using the assembly shown in Fig. 2 (a). CCR and COR testing are conducted using the assembly shown in Fig. 2 (b). In the former, the gear motor is connected to a solid penetrator directly. In the latter, the gear motor is connected to the cone through an inner

rod inside a hollow penetrator shaft. To achieve this, a 4 mm-to-8 mm rigid shaft coupler was used to convert the rotational movement of the gear motor to a 8 mm rotary rod. The rotary rod passes the hollow shaft and is locked by two ball bearings at the top and bottom of the shaft.

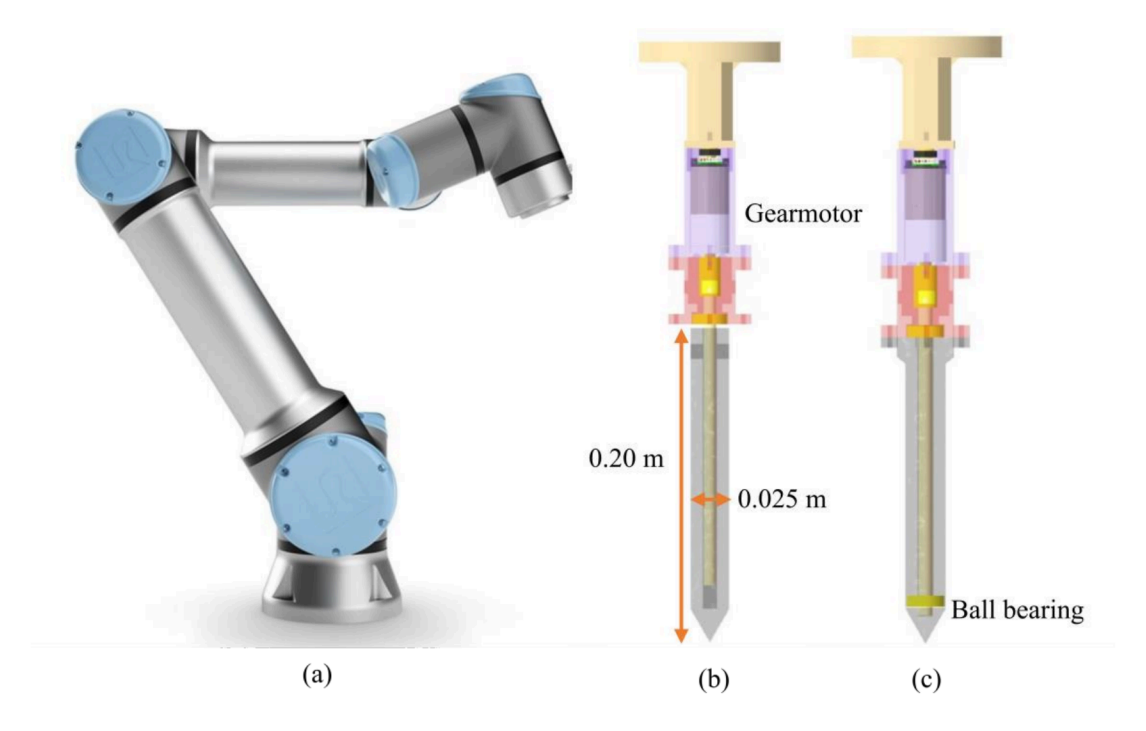


Fig. 2. Experimental setup for the rotational penetration tests: (a) Six-axis robotic arm (UR16e); (b) penetrator assembly for WCR tests; (c) penetrator assembly for CCR and COR tests.

Each penetrator assembly is connected to a flange of a six-axis robotic arm (UR16e, Fig. 2 a), which controls the vertical penetration and collects the force/displacement data. The rotational movement of the gear motor was controlled by a microcontroller (Arduino Mega). The proportional integral derivative (PID) control method was adopted to maintain the rotational speed and period of the gear motor here. A python library named Real-Time Data Exchange was used to transmit the recorded penetration force and torque data from the control box of the robotic arm into the local desktop.

A cylindrical bucket with a diameter of 28 cm and a depth of 36 cm was used to contain the Ottawa sand F65 ($D_{50} = 0.2$ mm). The soil sample is prepared by the dry pluviation method, and a relative density of 0.33 is achieved.

A series of rotational penetration tests were conducted with different combinations of vertical and rotational velocities while the resultant velocity was kept as a constant (Fig. 3). In Fig. 3, the length of each vector represents the magnitude of the resultant velocity, which is 0.04 m/s; the direction of each vector indicates the shearing direction. Different velocity combinations are indicated using the labeling convention "vertical velocity in m/s - rotational speed in revolution per minute (rpm)". For example, the (0.04 m/s - 0 rpm) case represents the direct penetration case (control case), and the (0.00 m/s - 30.56 rpm) case represents the pure rotational case. Each case was conducted for WCR, CCR, and COR, and each was tested three times to ensure the repeatability of the experiments.

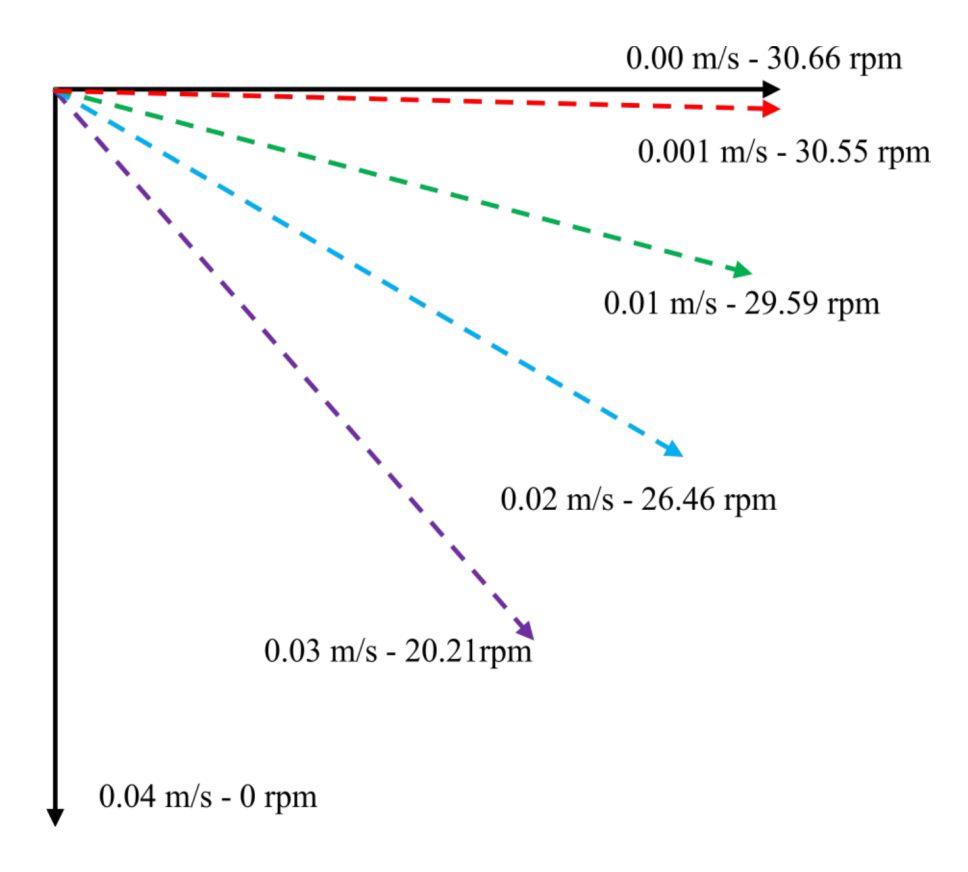


Fig. 3. Illustration of the combination of the velocities (The label indicates "vertical velocity – rotational velocity")

RESULTS

The total penetration force and torque on the penetrator under different rotational modes (WCR, CCR, and COR) and velocities were shown in Fig. 4, Fig. 5, and Fig. 6. Generally, the penetration force increases with the increasing penetration depth but decreases with the relative slip velocity, as shown in Fig. 4 (a), Fig. 5 (a), and Fig. 6 (a). At the same time, the penetration torque increases with the increase of the relative slip velocity, as shown in Fig. 4 (b), Fig. 5 (b), and Fig. 6 (b). The difference of the penetration torque between any two neighboring rotational cases within a testing group (WCR, CCR, or COR) becomes smaller, especially at the higher rotational velocities. Theoretically, there should be no resistive torque for the direct penetration case (0.04 m/s - 0 rpm, or the control case) if the soil sample is uniform and the penetration is perfectly vertical. The slightly negative torque for the control case in this study is likely attributed more to the slight inclination of the penetrator due to the reduced rigidity of the multicomponent assembly (Fig. 2 b). Nevertheless, the overall quality of the data is considered acceptable.

The penetration forces of the oscillatory cases under the same rotational velocities but different rotational degrees are shown in Fig. 7. It shows that, under the tested conditions, the rotational amplitude does not have a significant impact on the penetration force and torque (Fig. 7 a, b), highlighting the dominating role of relative slip velocity in reducing penetration forces.

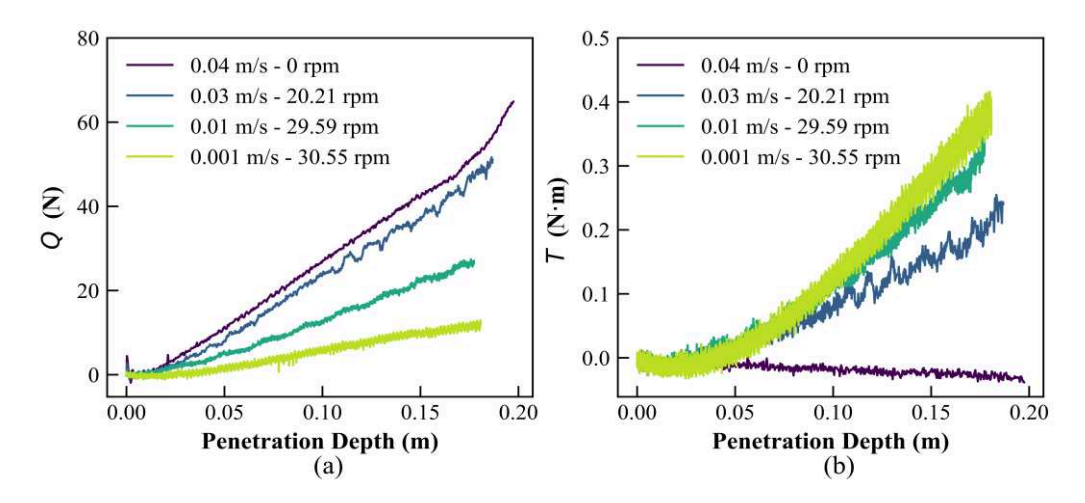


Fig. 4. Total penetration force and torque for WCR tests under different velocity combinations: (a) penetration force (Q); (b) penetration torque (T).

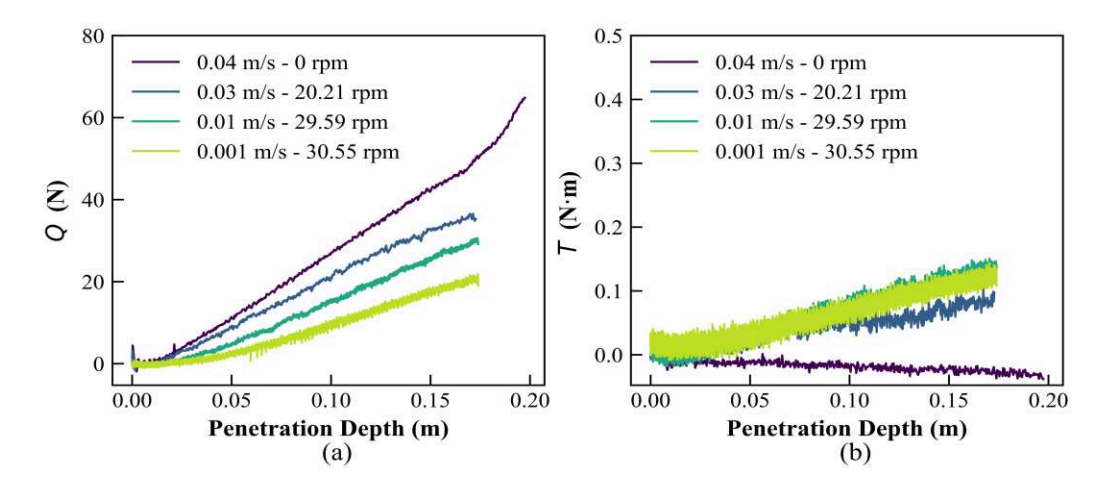


Fig. 5. Total penetration force and torque for CCR tests under different velocity combinations: (a) penetration force (Q); (b) penetration torque (T).

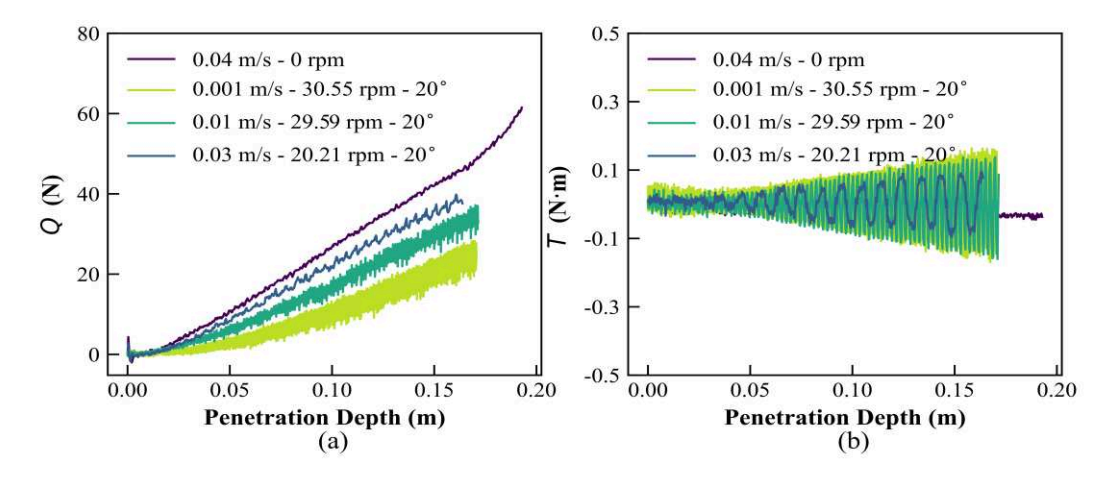


Fig. 6. Total penetration force and torque for COR tests under different velocity combinations: (a) penetration force (Q); (b) penetration torque (T).

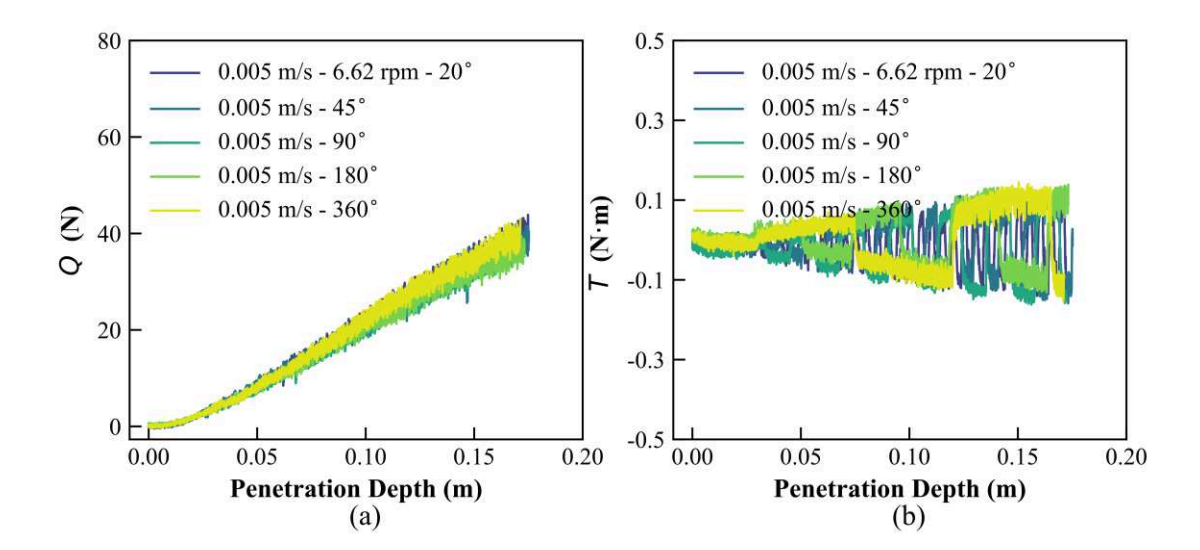


Fig. 7. Total penetration force and torque for COR tests under different rotational angles: (a) penetration force (Q); (b) penetration torque (T).

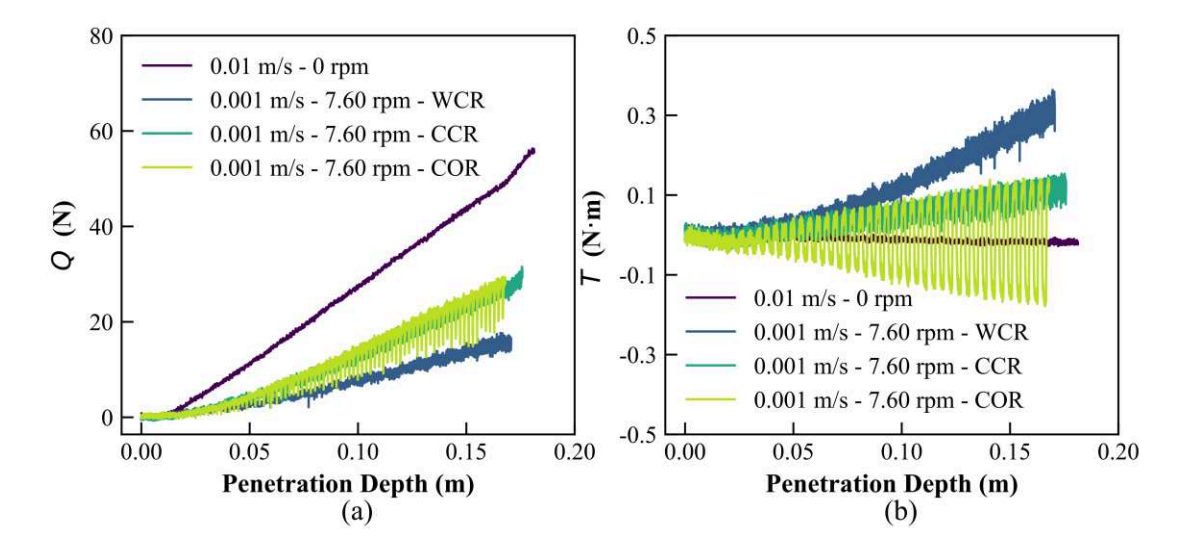


Fig. 8. Penetration force and torque with different rotational modes under the same velocity combinations: (a) penetration force (Q); (b) penetration torque (T) (The rotational degree for the selected COR case is 90°).

The effects of rotation mode and velocities on penetration force are better demonstrated when examined using non-dimensional metrics (Fig. 9). The normalized curves for three modes showed similar trends: the penetration force reduces dramatically with the relative slip velocity, until which reaches a critical value around 10 when the reductions start to plateau. Furthermore, the curves for the CCR and COR cases are almost identical to each other. The normalized penetration forces for all modes are close to each other when the relative slip velocity is less than 4. After that, the difference of the whole-body rotation case (WCR) and the cone-only rotation cases (CCR and COR) starts to increase.

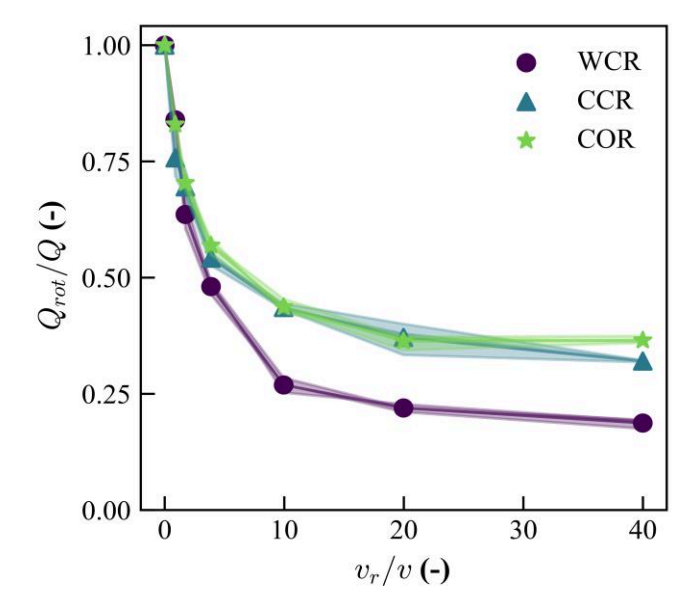


Fig. 9. The normalized penetration force Q_{rot}/Q for different rotational modes. Q indicates the penetration force for the direct penetration; Q_{rot} indicates the penetration force for the rotational penetration; v and v_r represent the vertical and rotational velocities, respectively. Each point was calculated by getting the normalized penetration force at every 0.05 m (0.05 m, 0.10 m, and 0.15 m) for each trial first and then averaging the normalized penetration force of the three trials under each case. Namely, the average value was calculated by averaging the values of nine points; the shaded area represents the difference between the average value of each case and the normalized penetration force for each trial under the same case.)

DISCUSSION

At the maximum relative slip ratio of 40 in this study, the penetration force reduced to about 30% of that in direct penetration when only the cone rotates during penetration; this number reduces to 20% when the whole penetrator rotates during penetration. The difference of 10% can thus be attributed to the effect of shaft rotation on the shaft resistance. It can also be concluded that when the whole penetrator rotates, the majority of the reduction of penetration force occurs at the cone.

The fact that continuous or oscillatory rotations have comparable effects on the reduction of penetration force implies that the forces resulting from continuous shearing and cyclic shearing under the test conditions in this study: shallow, dry, loose sand. This conclusion also underscores that a burrowing organism (such as the worm lizard) or robot does not have to perform continuous rotation to achieve the reduction of penetration force. Burrowing animals can certainly benefit from this since the rotational amplitude of a certain body part is almost always limited by the joints; and continuous rotation is not possible for most living organisms. For a burrowing robot, the oscillatory design may be simpler than a continuous rotation design since it can eliminate the use of a slipping ring. Whether this conclusion still holds for conditions involving different penetration depths, water contents, relative densities, and soil types warrants further investigation.

CONCLUSIONS

Different rotational modes including continuous or oscillatory, whole-body or cone-only rotations at different relative rotational speeds can all lead to a considerable reduction of the penetration force in shallow, dry, loose sand. With increasing relative slip velocity, the penetration force decreases while the penetration torque increases. With the same relative slip velocity, continuous and oscillatory cone-only rotations result in comparable effects on the change of penetration force and torque and rotational amplitude have negligible effects. On the other hand, whole-body continuous rotations result in greater reductions of penetration force and greater increases of penetration torque; the differences between whole-body rotation cases and cone-only rotation cases underscore the effect of rotating shaft on shaft penetration resistance, which is relatively small comparing with that of rotating cone on cone penetration resistance.

ACKNOWLEDGEMENT

This material is based upon work supported by the National Science Foundation (NSF) under NSF CMMI 1849674 and CMMI 1841574. Any opinions, findings, and conclusions or recommendations expressed in this material are those of the authors and do not necessarily reflect those of the NSF.

REFERENCES

- Abraham, Y., and R. Elbaum. 2013b. "Hygroscopic movements in Geraniaceae: The structural variations that are responsible for coiling or bending." *New Phytologist*, 199 (2): 584–594.
- Abraham, Y., and R. Elbaum. 2013a. "Hygroscopic movements in Geraniaceae: The structural variations that are responsible for coiling or bending." *New Phytologist*, 199 (2): 584–594.
- Cogger, H. G., R. G. Zweifel, and D. Kirshner. 1998. *Encyclopedia of reptiles & amphibians*. Weldon Owen.
- Dorgan, K. M. 2015. "The biomechanics of burrowing and boring." *Journal of Experimental Biology*, 218 (2): 176–183.
- Evangelista, D., S. Hotton, and J. Dumais. 2011. "The mechanics of explosive dispersal and self-burial in the seeds of the filaree, *Erodium Cicutarium* (Geraniaceae)." *Journal of Experimental Biology*, 214 (4): 521–529.
- Gans, C. 1968. "Relative Success of Divergent Pathways in Amphisbaenian Specialization." *The American Naturalist*, 102 (926): 345–362. The University of Chicago Press.
- Huang, S., and J. Tao. 2020. "Modeling Clam-inspired Burrowing in Dry Sand using Cavity Expansion Theory and DEM." *Acta Geotechnica*, 15 (8): 2305–2326.
- Maladen, R. D., Y. Ding, C. Li, and D. I. Goldman. 2009. "Undulatory Swimming in Sand: Subsurface Locomotion of the Sandfish Lizard." *Science*, 325 (5938): 314–318.
- Maladen, R. D., Y. Ding, P. B. Umbanhowar, and D. I. Goldman. 2011a. "Undulatory swimming in sand: Experimental and simulation studies of a robotic sandfish." *The International Journal of Robotics Research*, 30 (7): 793–805. SAGE Publications Ltd STM.
- Maladen, R. D., Y. Ding, P. B. Umbanhowar, A. Kamor, and D. I. Goldman. 2011b. "Mechanical models of sandfish locomotion reveal principles of high performance subsurface sand-swimming." *Journal of The Royal Society Interface*. The Royal Society.
- Migliaccio, F., P. Tassone, and A. Fortunati. 2013. "Circumnutation as an autonomous root movement in plants." *American Journal of Botany*, 100 (1): 4–13.

- Stamp, N. E. 1984. "Self-Burial Behaviour of Erodium Cicutarium Seeds." *Journal of Ecology*, 72 (2): 611–620. [Wiley, British Ecological Society].
- Tang, Y., and J. Tao. 2022a. "Multiscale analysis of rotational penetration in shallow dry sand and implications for self-burrowing robot design." *Acta Geotechnica*.
- Tang, Y., and J. J. Tao. 2022b. Effect of Rotational Cone on Penetration Resistance and Its Implication to the Design of a Bio-Inspired Self-Burrowing Robots. 214–222. American Society of Civil Engineers.
- Trueman, E. R., and M. Yonge. 1967. "The dynamics of burrowing in Ensis (Bivalvia)." *Proceedings of the Royal Society of London. Series B. Biological Sciences*, 166 (1005): 459–476. Royal Society.
- Winter, A. G., V. R. L. H. Deits, D. S. Dorsch, A. H. Slocum, and A. E. Hosoi. 2014. "Razor clam to RoboClam: Burrowing drag reduction mechanisms and their robotic adaptation." *Bioinspiration & Biomimetics*, 9 (3): 036009.